

Molecular Cancer Therapeutics



Next Generation Sequencing of Prostate Cancer from a Patient Identifies a Deficiency of Methylthioadenine Phosphorylase (MTAP), an Exploitable Tumor Target

Colin C Collins, Stanislav V Volik, Anna Lapuk, et al.

Mol Cancer Ther Published OnlineFirst January 17, 2012.

Updated Version

Access the most recent version of this article at:
doi:[10.1158/1535-7163.MCT-11-0826](https://doi.org/10.1158/1535-7163.MCT-11-0826)

Supplementary Material

Access the most recent supplemental material at:
<http://mct.aacrjournals.org/content/suppl/2012/01/16/1535-7163.MCT-11-0826.DC1.html>

Author Manuscript

Author manuscripts have been peer reviewed and accepted for publication but have not yet been edited.

E-mail alerts

[Sign up to receive free email-alerts](#) related to this article or journal.

Reprints and Subscriptions

To order reprints of this article or to subscribe to the journal, contact the AACR Publications Department at pubs@aacr.org.

Permissions

To request permission to re-use all or part of this article, contact the AACR Publications Department at permissions@aacr.org.

Next Generation Sequencing of Prostate Cancer from a Patient Identifies a Deficiency of Methylthioadenosine Phosphorylase (MTAP), an Exploitable Tumor Target

Authors and Affiliations

Colin C Collins¹, Stanislav V Volik¹, Anna V Lapuk¹, Yuwei Wang^{1,2}, Peter W Gout², Chunxiao Wu¹, Hui Xue^{1,2}, Hongwei Cheng^{1,2}, Anne Haegert¹, Robert H Bell¹, Sonal Brahmhatt¹, Shawn Anderson¹, Ladan Fazli¹, Antonio Hurtado-Coll¹, Mark A. Rubin³, Francesca Demichelis³, Himisha Beltran³, Martin Hirst², Marco Marra², Christopher A. Maher⁴, Arul M. Chinnaiyan⁴, Martin Gleave¹, Joseph R. Bertino⁵, Martin Lubin^{6a} & Yuzhuo Wang^{1,2}.

¹Vancouver Prostate Centre & Department of Urologic Sciences, University of British Columbia; ²BC Cancer Research Centre, BC Cancer Agency, Vancouver, BC, Canada; ³Weill Cornell Medical College, New York, NY, USA, ⁴Department of Pathology, University of Michigan, Ann Arbor, MI, USA, ⁵Cancer Institute of New Jersey, New Brunswick, NJ, USA, ⁶Dartmouth Medical School, Hanover NH, USA.

Running Title

Exploitation of NGS-detected MTAP deletion for PCa treatment

Keywords

massively parallel sequencing, MTAP, patient-derived xenograft, genitourinary cancers: prostate, animal models of cancer, gene expression profiling, functional genomics, xenograft models

Abbreviations list

MTA: 5'-Deoxy-5'-Methylthioadenosine, MTAP: Methylthioadenosine Phosphorylase, 6-TG: 6-Thioguanine, aCGH – array comparative genomic hybridization, CRPC: castrate resistant prostate cancer, MPS: massively parallel genome sequencing

Financial support

This study was supported by the Canadian Institutes of Health Research (YZW/MG), Centres of Excellence for Commercialization and Research (MG), and PNW Prostate SPORE P50 CA097186, Prostate Cancer Canada, and Genome BC (CC). YZW is a recipient of an Overseas Chinese Scholar Award from the National Natural Science Foundation of China (No 30928027), and a recipient of an Innovative Scholar Award from ICARE. The work in AC laboratory was supported by NIH P50 CA69568, U01 CA111275 and R01CA132874 grants.

Corresponding author

Colin C. Collins, Ph.D.

Mailing address: 2660 Oak Street, Vancouver, BC, Canada V6H 3Z6.

Cell phone: 604.779.9287. Fax: 604.875.5654

Email: ccollins@prostatecentre.com.

^a Possible conflict of interest

Potential conflict of interest

Dr. Martin Lubin has filed a patent application for using MTA/6-TG therapy in MTAP-deficient tumours.

Notes about the manuscript

Abstract: 189 words. Total word count (excluding references, including abstract and figure legends): 4498. Figures: 4. Supplemental figures: 1.

Abstract

Castrate resistant prostate cancer (CRPC) and neuroendocrine carcinoma of the prostate are invariably fatal diseases for which only palliative therapies exist. As part of a prostate tumour sequencing program, a patient tumour was analyzed using Illumina genome sequencing and a matched renal capsule tumour xenograft was generated. Both tumour and xenograft had a homozygous 9p21 deletion spanning the *MTAP*, *CDKN2* and *ARF* genes. It is rare for this deletion to occur in primary prostate tumours yet approximately 10% express decreased levels of *MTAP* mRNA. Decreased *MTAP* expression is a prognosticator for poor outcome. Moreover, it appears that this deletion is more common in CRPC than in primary prostate cancer. We show for the first time that treatment with methylthioadenosine and high dose 6-thioguanine causes marked inhibition of a patient derived neuroendocrine xenograft growth while protecting the host from 6-thioguanine toxicity. This therapeutic approach can be applied to other *MTAP*-deficient human cancers since deletion or hypermethylation of the *MTAP* gene occurs in a broad spectrum of tumours at high frequency. The combination of genome sequencing and patient-derived xenografts can identify candidate therapeutic agents and evaluate them for personalized oncology.

Introduction

Annually, in North America, prostate cancer is diagnosed in 220,000 men and kills approximately 35,000, making it the second leading cause of cancer-related deaths for men. It is estimated that one in six men will develop the disease in their lifetime. Prostate cancer grows most commonly as an adenocarcinoma with varying degrees of neuroendocrine differentiation (NED). Focal NED is observed at all stages of prostate cancer to various extents (30-100%) (1).

Pure neuroendocrine (NE) prostate cancers are rare but extraordinarily aggressive, resistant to therapy and associated with poor patient survival (2, 3). Small cell carcinoma of the prostate is a pathologic subtype of prostate cancer with unique clinical features and accounts for no more than 1% of all the prostatic malignancies. Typically they are discovered at an advanced stage or as recurrences of castration-resistant adenocarcinoma following treatment with hormonal therapy (4-8). In contrast to androgen-dependent adenocarcinoma of the prostate, small cell carcinomas do not usually express the androgen receptor (AR) or prostate specific antigen (PSA), but do frequently express NE markers such as Chromogranin A, Synaptophysin, CD56 and Neuron-specific Enolase (9, 10). Because NE prostate cancers do not express AR, they are not responsive to anti-androgens, rendering mainstream therapies for prostate cancer ineffective and making chemotherapy the dominant treatment option. Unfortunately, responses are short lived and NE prostate cancer is invariably fatal (11, 12) making identification of novel therapeutic targets and more effective therapies critical.

Whole genome sequencing of prostate tumours and patient-derived prostate tumour xenografts identified one patient with metastatic neuroendocrine prostate cancer that had a homozygous deletion of the methylthioadenosine phosphorylase (*MTAP*) gene and thus presented an opportunity to test a recently proposed treatment strategy that had been successfully used with a human T-cell leukemia xenograft (13).

The *MTAP* gene encodes an enzyme that plays a major role in the metabolism of polyamines, compounds important in the proliferation and development of mammalian cells (14-18); there is considerable evidence that *MTAP* also functions as a tumour suppressor (19, 20). Deletions of *MTAP* frequently occur in conjunction with deletion of *CDKN2A*, a gene that encodes, via

alternative processing, the tumour suppressor proteins p16^{ink4A} and p14^{ARF}, important in the regulation of *p53* and *Rb* pathways (21). Consistent with their regulatory functions, *MTAP* and *CDKN2A* genes/proteins are frequently found to be co-deleted in a wide range of cancers, including breast, endometrial, non-small cell lung and pancreatic cancers, gliomas, mesotheliomas, osteosarcomas, soft tissue sarcomas and T cell acute leukemias at frequencies ranging from 10%-75% (reviewed in (13)). In mantle cell lymphomas, mesotheliomas and gastrointestinal stromal cancers the *MTAP-CDKN2A* deletion is correlated with poor patient survival (14, 16, 22). The *MTAP* gene can also be silenced epigenetically, by promoter methylation, in malignant melanoma (23).

Over the past 30 years, several strategies to treat *MTAP*-deficient tumours have been suggested (13). Because *in vitro* evidence showed that *MTAP*-deficient tumours have increased sensitivity to inhibitors of *de novo* purine biosynthesis, one such inhibitor – L-alanosine – was tested in a broad clinical trial. This trial failed to show any objective response (13, 24). In a more recent proposal, MTA, the natural substrate of the enzyme *MTAP*, is administered with an antimetabolite – either an adenine analog, such as 2,6-diaminopurine, or a pyrimidine analog, such as the clinically approved drug 5-fluorouracil, or, as used in the present study, another clinically approved drug, the guanine analog 6-thioguanine (6-TG) (15). These analogs are phosphoribosylated in cells to toxic nucleotides with 5-phosphoribosyl-1-pyrophosphate (PRPP) as the donor of the phosphoribosyl group. In normal, *MTAP*-containing cells, MTA is cleaved by *MTAP* to 5-methylthioribose-1-phosphate (which is further metabolized to methionine) and to adenine. The MTA-derived adenine is phosphoribosylated by *APRT* to form AMP, consuming PRPP and hence competitively inhibiting phosphoribosylation of 6-TG to a toxic nucleotide, thus

protecting the normal cells. In MTAP-deficient tumour cells, adenine cannot be generated from the supplied MTA and the activation of 6-TG to its toxic nucleotide is not inhibited, resulting in toxicity to the tumour cells.

The combination of MTA and 6-TG was shown to permit administration of extremely high – even lethal – doses of 6-TG, to treat an MTAP-deficient human T-cell leukemia CCRF-CEM xenograft, while the normal host tissues of the mouse, which all have MTAP, were protected (13). This demonstration of successful application of the strategy in treating a haematological tumour suggested that MTA, combined with high dose 6-TG, might also be applicable to solid tumours. Such solid tumours have not been shown to respond to 6-TG, in a clinical setting, because the dose of permissible 6-TG has been limited by toxicity, primarily to bone marrow. The treatment strategy described here may have application to many different MTAP-deficient solid tumours.

We now report successful application of this approach to a subrenal capsule xenograft generated from a patient's neuroendocrine prostate tumour that was shown to have an *MTAP-CDKN2A* deletion via massively parallel genome sequencing (MPS).

Materials and Methods

Materials and animals

Chemicals, stains, solvents and solutions were obtained from Sigma-Aldrich Canada Ltd, Oakville, ON, Canada, unless otherwise indicated. Male 6- to 8-week old NOD/SCID mice were bred by the BC Cancer Research Centre Animal Resource Centre, BC Cancer Agency, Vancouver, Canada. Mice were housed in groups of three in microisolators with free access to

food and water and their health was monitored daily. Prostate cancer specimens were obtained at the Vancouver Prostate Centre, Vancouver General Hospital, with the patient's written and informed consent. The nature and consequences of the studies were explained. All experimental protocols were approved by the University of British Columbia Animal Care Committee. Ethical approval was provided by the University of British Columbia - British Columbia Cancer Agency Research Ethics Board (UBC BCCA REB #H04-60131).

Development of the LTL352 xenograft line: Use in 6-TG+MTA efficacy studies

Subrenal capsule xenografts were established from the patient's NE urethral metastatic tissue using routine methodology previously described (25). Briefly, fresh tumour tissue was collected and cut into $1 \times 2 \times 3 \text{ mm}^3$ pieces and then grafted under the renal capsules of six male NOD/SCID mice. Some of the rapidly growing grafts were maintained for up to five transplant generations by serial subrenal capsule transplantation into male NOD/SCID mice. A transplantable tumor tissue line, designated LTL352, was stored frozen with DMSO in liquid nitrogen for further use. For efficacy studies, LTL352 tissue was resurrected from liquid nitrogen storage and pieces of tissue were grafted into the subrenal capsule graft site of NOD/SCID mice to increase the amount of cancer tissue. After two months the tissues were harvested and cut into small pieces ($1 \times 2 \times 3 \text{ mm}^3$) and then grafted *subcutaneously* into 18 male NOD/SCID mice. After 5 weeks (to allow enlargement of the grafts $>100 \text{ mm}^3$) the 18 mice were randomly distributed into three groups (6 mice per group) and treated (i.p.) on days 1, 5 and 9 with (i) 6-TG, (ii) 6-TG+MTA, and (iii) similar volumes of saline (controls). Tumor sizes were measured with calipers (mm) on days 1, 5, 9 and 12; all xenografts were harvested on day 12.

Histology and immunohistochemistry

Human prostate tissue samples and xenograft tissues were fixed in 10% neutral-buffered formalin and embedded in paraffin. Serial sections (5 μm thick) were cut on a microtome, mounted on glass slides, de-waxed in HistoClear (National Diagnostic, Atlanta, GA) and then hydrated in graded alcohol solutions and distilled water. One slide was stained with hematoxylin and eosin for histological characterization and adjacent sections of each tissue sample were used for immunohistochemical (IHC) staining. For IHC staining, endogenous peroxidase activity was blocked with 0.5% hydrogen peroxide in methanol for 10 minutes followed by washing with PBS (pH 7.4). Blocking solution (ImmunoVision Technology, Springdale, AR, USA) was applied to the sections for 60 minutes to block nonspecific sites. The sections were then incubated with primary antibodies overnight at 4°C. Following incubation with the primary antibodies, sections were washed with PBS and incubated for 30 min at room temperature with the appropriate biotinylated secondary antibodies and then incubated with avidin–biotin complex (Vector Laboratories, Foster City, CA) for 30 min at room temperature. Immunoreactivity was visualized using 3,3'-diaminobenzidine tetrahydrochloride (DAB) reaction. Sections were counterstained with hematoxylin and dehydrated in graded alcohols. Primary antibodies used included rabbit anti-synaptophysin (SYN; Abcam Inc, Cambridge, MA); mouse anti-Ki-67 (DAKO; 1:50); rabbit anti-caspase-3 (Cell Signaling, Danvers, MA; 1:100); mouse anti-human P63 monoclonal and rabbit anti-human AR polyclonal antibody (Santa Cruz Biotechnology, Santa Cruz, CA). Control sections were processed in parallel with mouse or rabbit non-immune IgG (Dako) used at the same concentrations as the primary antibodies.

Quantification of Caspase-3 Positive Cells

For quantification of caspase-3 immunostaining of cells, five randomly selected high-power (X400) images from each graft were captured using an AxioCam HRCCD mounted on an AxioPlan 2 microscope, using Axiovision 3.1 software (Carl Zeiss). The percentages of caspase-3-positive cells were calculated using the formula: $\text{Percentage} = \frac{\text{number of positive cells} \times 100}{\text{number of total cells}}$. Viable tumour areas of the treated and control groups were averaged and presented as means \pm S.D. P-values were calculated using a permutation test of the means. Caspase-3 percentages are presented as means \pm S.D. and analyzed by the Student's t-test. Results with P-values <0.05 are considered statistically significant.

Tissue Microarrays Used

Tissue microarrays used in this study were constructed as described in (26). Gleason microarray contains tissue 1mm cores from 88 patients with Gleason grade from 3 to 5 spotted in duplicate (176 cores total). CRPC array contains 1mm cores from 12 CRPC patients spotted in duplicate (24 cores in total).

DNA sequencing

Sequencing of the original urethra tumour specimen used for LTL-352 xenograft was performed at BCCA Genome Sciences Centre in Vancouver, BC according to established protocols as described in (27). Approximately 100 million reads were obtained and mapped to the NCBI 36.1 human genome reference sequence using MAQ 0.7.1(28) and the following parameters: $-n\ 1\ -N\ -e\ 100\ -a\ 700$. The total number of sequenced bases in a given genomic window and the average sequencing depth across the window (10 or 30 kb) was then calculated. The copy number was

approximated by the ratio of average sequencing depth in a given window to the average sequencing depth across the genome. This value was transformed into log₂ space. Copy number profiles were visualized and copy number abnormalities (CNAs) associated with resistance phenotype identified using the NexusCGH software package (Biodiscovery Inc.).

Array CGH

Digestion of snap-frozen tumour tissue with 0.2 mg/ml Proteinase K (Roche, Laval, QC, Canada) in digestion buffer (50 mM NaCl, 10 mM Tris-HCl (pH 8.3), 1 mM EDTA and 0.5% SDS) was carried out overnight at 55°C. The cell lysates were purified by Phenol:Chloroform:Isoamyl Alcohol (25:24:1), and DNA was precipitated by adding 1/10th volume of 3M sodium acetate and 2.5 volumes of 100% ethanol at -20°C. The DNA was re-suspended in water at 37°C for 1 hour. 0.5 µg of tumour and male reference genomic DNA (Promega Corp) was fluorescently labeled by following the NimbleGen enzymatic labeling protocol which employs Cy3 and Cy5 labeled random nanomers (TriLink Biotechnologies), a heat fragmentation step at 98°C for 10 minutes, and amplification with Klenow fragment 5'-3'exo- (NEB). 5 µg of each Cy5-labeled sample was co-hybridized with 5 µg of Cy3-labeled human male reference DNA (Promega Corp) on Agilent SurePrint G3 Human Catalog CGH 4x180K (Part No. G4449A) following the hybridization and washing conditions from the Agilent Oligonucleotide Array-Based CGH for Genomic DNA Analysis Protocol v6.2. Arrays were scanned with the Agilent DNA Microarray Scanner and quantified with Feature Extraction 10.5.1.1. CGH processed signal was then uploaded into Biodiscovery Nexus CGH v. 5.1 software, where the quality was assessed and data were visualized and analyzed.

Results

Small cell carcinoma of the prostate expressing neuroendocrine markers

A 77-year old Caucasian male patient (#946) was diagnosed with a metastatic prostatic adenocarcinoma with a Gleason score of 5+4 = 9. At the time of diagnosis, his serum PSA level was 14 ng/ml. The patient was treated with continuous androgen ablation therapy (zoladex and casodex combination). Forty months later he developed, despite a good initial response, a large local recurrence and a bladder outlet obstruction and was treated with palliative radiotherapy. Tumour growth resumed within two months and the patient developed bleeding and urinary retention and underwent a palliative cystoprostatectomy. Pathology revealed poorly differentiated carcinoma extending into the seminal vesicle, bladder neck and the right ureter. Two months later, and four years after his initial diagnosis, palpable metastatic lesions were excised from his bulbar urethra and corpora cavernosa showing extensive involvement of small cell carcinoma infiltrating smooth muscle with the expression of typical NE markers, i.e. CD56, Chromogranin A and Synaptophysin (Fig. 1) and absence of expression of AR and TP63 (Supplemental Figure 1).

Genome sequencing of patient's tumour identifies a 9p21 MTAP-CDKN2A deletion

In an effort to identify therapeutic strategies based on the genotype of this patient's tumour, we sequenced the genome of the urethral NE metastasis using Illumina massively parallel sequencing (MPS) (29). We converted approximately 100 million mapped paired-end sequence reads to copy number data and visualized the resulting copy number plots using Biodiscovery Nexus CGH software. This process revealed a highly rearranged tumour genome showing a

homozygous deletion in chromosome 9p21 (Fig 2). Inspection of the 9p21 deletion confirmed that it was homozygous and showed that it had a size of 450 kilobases and encompassed the *MTAP* and cyclin-dependent kinase inhibitor 2A (*CDKN2A*) genes, as well as two other genes, i.e. the doublesex and mab-3 related transcription factor 1 (*DMRTA1*) and the embryonic lethal, abnormal vision (*ELAVL2*) genes. Sequencing the transcriptome of the patient's NE prostate cancer metastasis revealed that *MTAP* and *CDKN2A* transcripts could be detected but at very low levels, presumably reflecting a combination of infiltrating macrophages, tumour heterogeneity and stromal admixture (Fig. 3).

Patient's tumour xenograft line has the same 9p21 MTAP-CDKN2A deletion

In parallel with DNA sequencing, a transplantable subrenal capsule xenograft line, LTL352, was successfully established from the patient's NE urethral metastasis. The subrenal location for xenografts was chosen because our past experience showed that this grafting site is ideal for establishing patient-derived xenografts (25, 30-32). All the grafts started to grow after a latency period of about three months. The tumour volume doubling time of LTL352 in NOD/SCID mice was about 11 days. The phenotype of the original cancer was retained throughout the serial transplantations, as indicated by its histology and in particular by the expression of the NE marker, synaptophysin (Fig. 1) and absence of expression of AR and TP63 (Supplemental Fig. 1). Furthermore, as shown by array comparative genomic hybridization (aCGH), the LTL352 xenograft line had the same 9p21 *MTAP-CDKN2A* deletion as the patient's tumour (Fig. 2). LTL352 also had the lowest *MTAP* expression according to qPCR (Fig. 3B).

Effect of 6-TG ± MTA treatment on LTL352 xenograft growth

Groups of NOD/SCID mice carrying *subcutaneous* LTL352 xenografts (size 100-160 mm³) were treated (i.p.) during a 12-day period (on days 1, 5, 9) with 6-TG (75 mg/kg, seven mice), 6-TG + MTA (75 mg/kg and 100 mg/kg respectively, seven mice), or saline (controls, five mice). As shown in Figure 4A, the growth of the xenografts was markedly inhibited by 6-TG+MTA. In the control group, the average tumour volume increased over the 12-day period from 150±22 mm³ to 315±48 mm³ (mean ± standard error of mean) - an increase of about 110%. In the 6-TG+MTA group the tumour volume increased only slightly from 134±12 mm³ to 182±18 mm³ - an increase of about 36%. This amounts to a 6-TG+MTA-induced growth inhibition (the percentage increase of tumour volume of treated tumours compared with the controls) of 74% ($P<0.05$).

Administration of 6-TG on its own was highly toxic resulting in the death of all 6-TG-treated mice within 12 days, whereas none of the mice treated with 6-TG+MTA showed significant weight loss. Histopathological analysis was used to determine the effect of the drugs at the cellular level. A comparison with the control tissues showed that the tissues of 6-TG+MTA-treated tumours contained more apoptotic bodies (Fig. 4B). Furthermore, a marked increase was found for the staining of Caspase-3 (a marker of apoptosis) for the 6-TG+MTA-treated group (Fig. 4B) – 6-TG+MTA xenografts had 4.49±0.26% (mean ± S.D.) of caspase-3 positive cells – a highly significant ($p<0.0001$) increase over the control group's 1.42±0.17% (mean ± S.D.) - in line with reported induction of apoptosis by 6-TG (33). Also, Ki-67 activity (a marker of cell proliferation) was reduced in the 6-TG+MTA-treated tumours ($p<0.01$, data not shown) compared to the control group. Taken together, the results indicate that addition of MTA to 6-TG was effective in protecting the host from 6-TG toxicity thus enhancing specific targeting of the malignancy.

It should be noted that the choice of 12 day study duration was prompted by two considerations. Firstly, the doubling time of LTL352 is approximately 11 days. Secondly, the approved animal protocol limits the final sum of tumour volume in the mouse by 1000 mm³. Therefore, we had to ensure, that the volume of each graft would not exceed 350 mm³, since there are two to three grafts per mouse.

We have sequenced the genomes of 20 high risk prostate tumours at the Vancouver Prostate Centre and found *MTAP* to be deleted in 30% of them. In independent cohorts analyzed using Affymetrix SNP arrays *MTAP* was found to be deleted in 10% (3/30) and 70% (5/7) of prostatic adenocarcinomas and neuroendocrine tumours, respectively. Finally, we find *MTAP* deletion to occur significantly ($p=0.027$, Fisher's exact test) more often in CRPC tumour samples on a VPC CRPC tissue microarray (three out of 12 patients have deletions) compared to Gleason 2009 array (where deletion was detected in two out of 78 patients). We also find *MTAP* to be significantly ($p= 0.036$, Fisher's exact test) more often deleted in GEO GSE14996 dataset that contains Affymetrix SNP6.0-based copy number profiles of multisampled metastatic prostate tumours (34) (three out of 14 patients have deletions) compared to VPC Gleason 2009 TMA. In the majority of these tumours *MTAP* is heterozygously deleted and *MTAP* expression correlates well with copy number (Fig. 3C). To understand the clinical significance of this we analyzed gene expression data for 230 prostate tumours (accessible at cBio Cancer Genomics Portal developed by the Computational Biology Center at Memorial Sloan-Kettering Cancer Center) (35) and found that *MTAP* expression is decreased by more than 2 Z-scores in approximately 11% of tumours. Moreover, a Kaplan-Meier analysis revealed that *MTAP* expression is associated with significantly shorter time to post-operative recurrence as measured by prostate

specific antigen (Figure 3D). Thus, reduced expression of *MTAP* appears to be both prognostic and predictive for *MTAP* based therapies.

Discussion

To gain insight into the molecular mechanisms driving prostate tumour progression, and to devise novel therapeutic strategies, we routinely sequence prostate tumour genomes and/or transcriptomes from selected patients. This approach led to the finding that the NE small cell carcinoma presented in this study had a homozygous *MTAP-CDKN2A* deletion as shown by MPS and confirmed by aCGH (Fig. 2). The absence of *MTAP* in the tumour motivated experimentation to determine if it might respond to a therapeutic strategy first advanced by Lubin and Lubin (15), based on use of a high dose of a *purine* analog, such as 6-TG, in combination with MTA. In normal host cells this combination competitively inhibits conversion of 6-TG to its toxic nucleotide and as such can protect the host from 6-TG toxicity. But in *MTAP*-deficient tumour cells, MTA does not protect the tumour from 6-TG toxicity, and the tumour is inhibited or is killed. This selective strategy was previously found to be effective for treatment of the human T-cell leukemia, CCRF-CEM, in a mouse xenograft model, while the host mouse tissues were protected by MTA from 6-TG toxicity (13).

Development of new drugs has been seriously hampered by the lack of clinically relevant, experimental *in vivo* cancer models required for drug efficacy evaluation. Only about 5% of potential new anti-cancer agents, that have successfully passed all required preclinical tests, have efficacy in clinical trials and are approved for clinical usage by the U.S. Food and Drug Administration (36). There is therefore a critical need for experimental models with improved ability to predict clinical drug efficacy (37). To overcome this hurdle we have recently developed

transplantable, patient-derived tumour *tissue* xenografts that have very high engraftment rates (>95%) in NOD/SCID mice and closely resemble the original cancers in histopathology, biomarker expression and genetic profiles (25, 32, 38-41). The LTL352 subrenal capsule xenograft line established from the patient's tumour closely resembles the patient's tumour particularly with regard to expression of the NE marker, synaptophysin (Fig. 1), and the 9p21 *MTAP-CDKN2A* deletion (Fig. 2). That the 6-TG+MTA treatment indeed had an inhibitory effect on the solid tumour xenografts was demonstrated by the marked reduction in their growth rate (Fig. 4A), by decreases in Ki67 expression (data not shown) and increases in caspase-3 expression and apoptotic bodies in the cancer cells (Fig. 4B). The protective effect of MTA was evident from the lack of weight loss of the 6-TG+MTA treated mice in contrast to the 6-TG-treated mice for which treatment with 6-TG, in the absence of MTA, was lethal.

While further optimization of dose and scheduling is needed to increase the growth-inhibitory effect, these studies show clearly that significant *in vivo* growth inhibition of *MTAP*-deficient solid tumours can be obtained, without toxicity to the host, by using 6-TG in combination with MTA. This combination therapy should be especially useful for cancers without effective therapy. As MTA has been given safely to humans, we are planning clinical trials using this strategy in patients with tumours lacking *MTAP*. Unfortunately, in the case of the tissue donor for this study, he continued to require palliative treatments for local and metastatic progression over the following 18 months before dying of metastatic prostate cancer.

To our knowledge, this is the first study to directly implicate loss of *MTAP* in prostate cancer and to associate it with the invariably fatal CRPC. Moreover this is one of the first studies to exploit whole genome sequencing for identification of a molecular target in a patient's tumour in

conjunction with *in vivo* evaluation of the target-related therapy using a patient derived xenograft of the patient's cancer. The latter could be especially useful for personalized cancer therapy.

Grant Support

This study was supported by the Canadian Institutes of Health Research (YZW/MG), Centres of Excellence for Commercialization and Research (MG), and PNW Prostate SPORE P50 CA097186, Prostate Cancer Canada, and Genome BC (CC). YZW is a recipient of an Overseas Chinese Scholar Award from the National Natural Science Foundation of China (No 30928027), and a recipient of an Innovative Scholar Award from ICARE. The work in AC laboratory was supported by NIH P50 CA69568, U01 CA111275 and R01CA132874 grants.

References

1. di Sant'Agnese PA. Neuroendocrine differentiation in carcinoma of the prostate. Diagnostic, prognostic, and therapeutic implications. *Cancer*. 1992;70:254-68.
2. Abbas F, Civantos F, Benedetto P, Soloway MS. Small cell carcinoma of the bladder and prostate. *Urology*. 1995;46:617-30.
3. Randolph TL, Amin MB, Ro JY, Ayala AG. Histologic variants of adenocarcinoma and other carcinomas of prostate: pathologic criteria and clinical significance. *Mod Pathol*. 1997;10:612-29.
4. Erasmus CE, Verhagen WI, Wauters CA, van Lindert EJ. Brain metastasis from prostate small cell carcinoma: not to be neglected. *Can J Neurol Sci*. 2002;29:375-7.
5. Miyoshi Y, Uemura H, Kitami K, Satomi Y, Kubota Y, Hosaka M. Neuroendocrine differentiated small cell carcinoma presenting as recurrent prostate cancer after androgen deprivation therapy. *BJU Int*. 2001;88:982-3.

6. Tanaka M, Suzuki Y, Takaoka K, Suzuki N, Murakami S, Matsuzaki O, et al. Progression of prostate cancer to neuroendocrine cell tumor. *Int J Urol*. 2001;8:431-6; discussion 7.
7. Papandreou CN, Daliani DD, Thall PF, Tu SM, Wang X, Reyes A, et al. Results of a phase II study with doxorubicin, etoposide, and cisplatin in patients with fully characterized small-cell carcinoma of the prostate. *J Clin Oncol*. 2002;20:3072-80.
8. Spieth ME, Lin YG, Nguyen TT. Diagnosing and treating small-cell carcinomas of prostatic origin. *Clin Nucl Med*. 2002;27:11-7.
9. Abrahamsson PA. Neuroendocrine differentiation in prostatic carcinoma. *Prostate*. 1999;39:135-48.
10. Bonkhoff H. Neuroendocrine cells in benign and malignant prostate tissue: morphogenesis, proliferation, and androgen receptor status. *Prostate Suppl*. 1998;8:18-22.
11. Helpap B. Morphology and therapeutic strategies for neuroendocrine tumors of the genitourinary tract. *Cancer*. 2002;95:1415-20.
12. Moore SR, Reinberg Y, Zhang G. Small cell carcinoma of prostate: effectiveness of hormonal versus chemotherapy. *Urology*. 1992;39:411-6.
13. Bertino JR, Waud WR, Parker WB, Lubin M. Targeting tumors that lack methylthioadenosine phosphorylase (MTAP) activity: Current strategies. *Cancer Biol Ther*. 2011;11:627-32.
14. Marce S, Balague O, Colomo L, Martinez A, Holler S, Villamor N, et al. Lack of methylthioadenosine phosphorylase expression in mantle cell lymphoma is associated with shorter survival: implications for a potential targeted therapy. *Clin Cancer Res*. 2006;12:3754-61.

15. Lubin M, Lubin A. Selective killing of tumors deficient in methylthioadenosine phosphorylase: a novel strategy. *PLoS One*. 2009;4:e5735.
16. Krasinskas AM, Bartlett DL, Cieply K, Dacic S. CDKN2A and MTAP deletions in peritoneal mesotheliomas are correlated with loss of p16 protein expression and poor survival. *Mod Pathol*. 2010;23:531-8.
17. Basu I, Cordovano G, Das I, Belbin TJ, Guha C, Schramm VL. A transition state analogue of 5'-methylthioadenosine phosphorylase induces apoptosis in head and neck cancers. *J Biol Chem*. 2007;282:21477-86.
18. Basu I, Locker J, Cassera MB, Belbin TJ, Merino EF, Dong X, et al. Growth and metastases of human lung cancer are inhibited in mouse xenografts by a transition state analogue of 5'-methylthioadenosine phosphorylase. *J Biol Chem*. 2011;286:4902-11.
19. Christopher SA, Diegelman P, Porter CW, Kruger WD. Methylthioadenosine phosphorylase, a gene frequently codeleted with p16(cdkN2a/ARF), acts as a tumor suppressor in a breast cancer cell line. *Cancer Res*. 2002;62:6639-44.
20. Kirovski G, Stevens AP, Czech B, Dettmer K, Weiss TS, Wild P, et al. Down-Regulation of Methylthioadenosine Phosphorylase (MTAP) Induces Progression of Hepatocellular Carcinoma via Accumulation of 5'-Deoxy-5'-Methylthioadenosine (MTA). *Am J Pathol*. 2011;178:1145-52.
21. Clurman BE, Groudine M. The CDKN2A tumor-suppressor locus--a tale of two proteins. *N Engl J Med*. 1998;338:910-2.

22. Huang HY, Li SH, Yu SC, Chou FF, Tzeng CC, Hu TH, et al. Homozygous deletion of MTAP gene as a poor prognosticator in gastrointestinal stromal tumors. *Clin Cancer Res.* 2009;15:6963-72.
23. Behrmann I, Wallner S, Komyod W, Heinrich PC, Schuierer M, Buettner R, et al. Characterization of methylthioadenosin phosphorylase (MTAP) expression in malignant melanoma. *Am J Pathol.* 2003;163:683-90.
24. Kindler HL, Burris HA, 3rd, Sandler AB, Oliff IA. A phase II multicenter study of L-alanosine, a potent inhibitor of adenine biosynthesis, in patients with MTAP-deficient cancer. *Invest New Drugs.* 2009;27:75-81.
25. Wang Y, Revelo MP, Sudilovsky D, Cao M, Chen WG, Goetz L, et al. Development and characterization of efficient xenograft models for benign and malignant human prostate tissue. *Prostate.* 2005;64:149-59.
26. Cox ME, Gleave ME, Zakikhani M, Bell RH, Piura E, Vickers E, et al. Insulin receptor expression by human prostate cancers. *Prostate.* 2009;69:33-40.
27. Shah SP, Morin RD, Khattra J, Prentice L, Pugh T, Burleigh A, et al. Mutational evolution in a lobular breast tumour profiled at single nucleotide resolution. *Nature.* 2009;461:809-13.
28. Li H, Ruan J, Durbin R. Mapping short DNA sequencing reads and calling variants using mapping quality scores. *Genome Res.* 2008;18:1851-8.
29. Zhao J, Grant SF. Advances in whole genome sequencing technology. *Curr Pharm Biotechnol.* 2011;12:293-305.

30. Lin D, Watahiki A, Bayani J, Zhang F, Liu L, Ling V, et al. ASAP1, a gene at 8q24, is associated with prostate cancer metastasis. *Cancer Res.* 2008;68:4352-9.
31. Tung WL, Wang Y, Gout PW, Liu DM, Gleave M. Use of irinotecan for treatment of small cell carcinoma of the prostate. *Prostate.* 2011;71:675-81.
32. Wang Y, Xue H, Cutz JC, Bayani J, Mawji NR, Chen WG, et al. An orthotopic metastatic prostate cancer model in SCID mice via grafting of a transplantable human prostate tumor line. *Lab Invest.* 2005;85:1392-404.
33. Karran P, Attard N. Thiopurines in current medical practice: molecular mechanisms and contributions to therapy-related cancer. *Nat Rev Cancer.* 2008;8:24-36.
34. Liu W, Laitinen S, Khan S, Vihinen M, Kowalski J, Yu G, et al. Copy number analysis indicates monoclonal origin of lethal metastatic prostate cancer. *Nat Med.* 2009;15:559-65.
35. Taylor BS, Schultz N, Hieronymus H, Gopalan A, Xiao Y, Carver BS, et al. Integrative genomic profiling of human prostate cancer. *Cancer Cell.* 2010;18:11-22.
36. Sharpless NE, Depinho RA. The mighty mouse: genetically engineered mouse models in cancer drug development. *Nat Rev Drug Discov.* 2006;5:741-54.
37. Voskoglou-Nomikos T, Pater JL, Seymour L. Clinical predictive value of the in vitro cell line, human xenograft, and mouse allograft preclinical cancer models. *Clin Cancer Res.* 2003;9:4227-39.
38. Lee CH, Xue H, Sutcliffe M, Gout PW, Huntsman DG, Miller DM, et al. Establishment of subrenal capsule xenografts of primary human ovarian tumors in SCID mice: potential models. *Gynecol Oncol.* 2005;96:48-55.

39. Cutz JC, Guan J, Bayani J, Yoshimoto M, Xue H, Sutcliffe M, et al. Establishment in severe combined immunodeficiency mice of subrenal capsule xenografts and transplantable tumor lines from a variety of primary human lung cancers: potential models for studying tumor progression-related changes. *Clin Cancer Res.* 2006;12:4043-54.
40. Andersen RJ, Mawji NR, Wang J, Wang G, Haile S, Myung JK, et al. Regression of castrate-recurrent prostate cancer by a small-molecule inhibitor of the amino-terminus domain of the androgen receptor. *Cancer Cell.* 2010;17:535-46.
41. Kortmann U, McAlpine JN, Xue H, Guan J, Ha G, Tully S, et al. Tumor growth inhibition by olaparib in BRCA2 germline-mutated patient-derived ovarian cancer tissue xenografts. *Clin Cancer Res.* 2011;17:783-91.

Figure Legends

Figure 1 (A) Immunohistochemical staining of tumour 946 tissue sections shows expression of neuroendocrine markers CD56, Chromogranin A and Synaptophysin, identifying the neuroendocrine origin of the tissue. **(B)** Synaptophysin staining of xenograft LTL352 tissue.

Figure 2 Comparison of chromosome 9p copy number profiles of the neuroendocrine urethra metastasis from patient #946 and its xenograft, LTL352, as produced by Illumina sequencing (MPS) and Agilent aCGH technologies. Array CGH confirmed that the deletion in the original tumor by MPS was real and not a mapping artifact, and that the patient's tumour and xenograft had the same deletion. Copy number profiles were visualized using NexusCGH (Biodiscovery,

Inc.). The *MTAP* deletion is expanded in the bottom panel (UCSC). Three additional genes mapping to this deletion are cyclin-dependent kinase inhibitor 2A (*CDKN2A*), doublesex and mab-3 related transcription factor 1 (*DMRTA1*) and embryonic lethal, abnormal vision (*ELAVL2*).

Figure 3 Expression of genes mapping within the 9p21 *MTAP* deletion. **(A)** RNA Sequence-derived expression data for *MTAP*, *CDKN2A*, *DMRTA1*, and *ELAVL2* – genes located within the minimal deletion at the *MTAP* locus. Expression levels were normalized to GAPDH. All samples had normal copy numbers of the *MTAP* locus with the exception of 946 and 972 urethra and penile metastases, respectively. Only the expression of *MTAP* shows essentially perfect correlation with the copy number. **(B)** Quantitative RT-PCR was performed to confirm this interpretation of the RNA-sequence data and to confirm concordance between 946 and 352. **(C)** *MTAP* expression levels determined in a Sloan-Kettering prostate cancer cohort (35). The cBio Cancer Genomics Portal was used for data access (http://www.cbioportal.org/cgx/?cancer_type_id=pca). The *MTAP* expression levels correlate well with the reduced copy numbers of *MTAP* locus. **(D)** Kaplan-Meier plot showing differences in time to recurrence as measured by PSA for the 26 patients with *MTAP* expression differing from the mean by a z-score of 2.0 or greater compared to the rest of the cohort. Decreased *MTAP* expression is significantly correlated with a shorter time to disease recurrence.

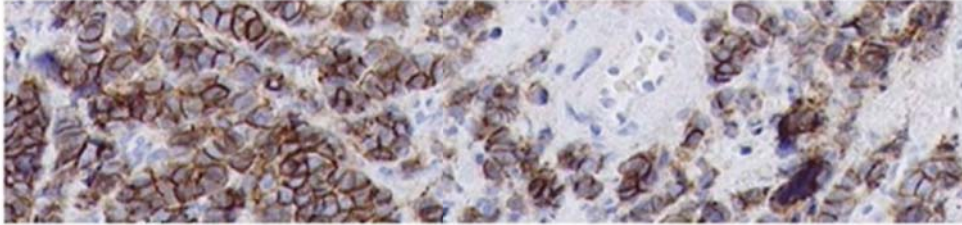
Figure 4 (A) Mice carrying LTL352 xenografts were treated (i.p.) with 6-TG (75 mg/kg)+MTA (100 mg/kg) or saline (controls) on days 1, 5 and 9. On day 12, the tumours in the treated group were approximately 64% smaller than those in the untreated control group (a decrease of tumour growth rate by about 74%). Mean values with standard errors of mean are plotted. * indicates

significant differences between control and treated tumours (paired t-test, $p < 0.05$). All mice treated with 6-TG in the absence of MTA died within 12 days. **(B)** Histological and immunohistochemical analysis of LTL352 tissues from control (untreated) and 6-TG+MTA-treated xenografts. Representative fields of H&E and Caspase-3 staining are shown. In the treated mice the tumours had reduced proliferation and increased apoptosis when compared to the control tumours as illustrated by increase of Caspase-3 positive cells from $1.42 \pm 0.17\%$ to $4.49 \pm 0.26\%$ (mean \pm S.D.). **(C)** The chemical structure of 5'-Deoxy-5'-Methylthioadenosine (MTA). **(D)** The chemical structure of 6-Thioguanine (6-TG).

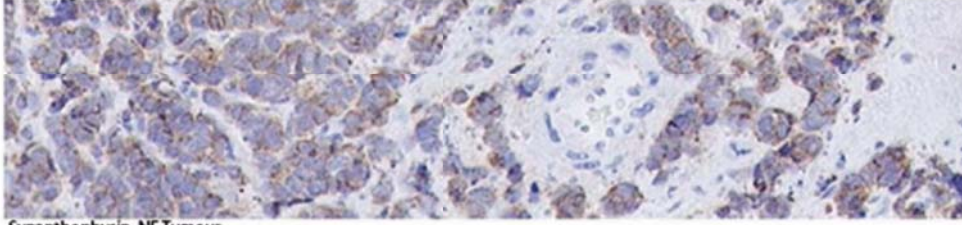
Figure 1

A.

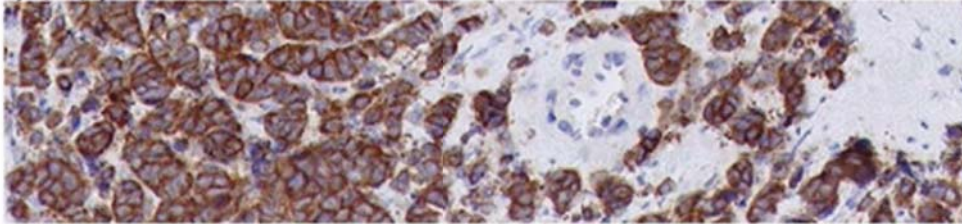
CD56 NE Tumour



ChromograninA NE Tumour



Synapthophysin NE Tumour



B.

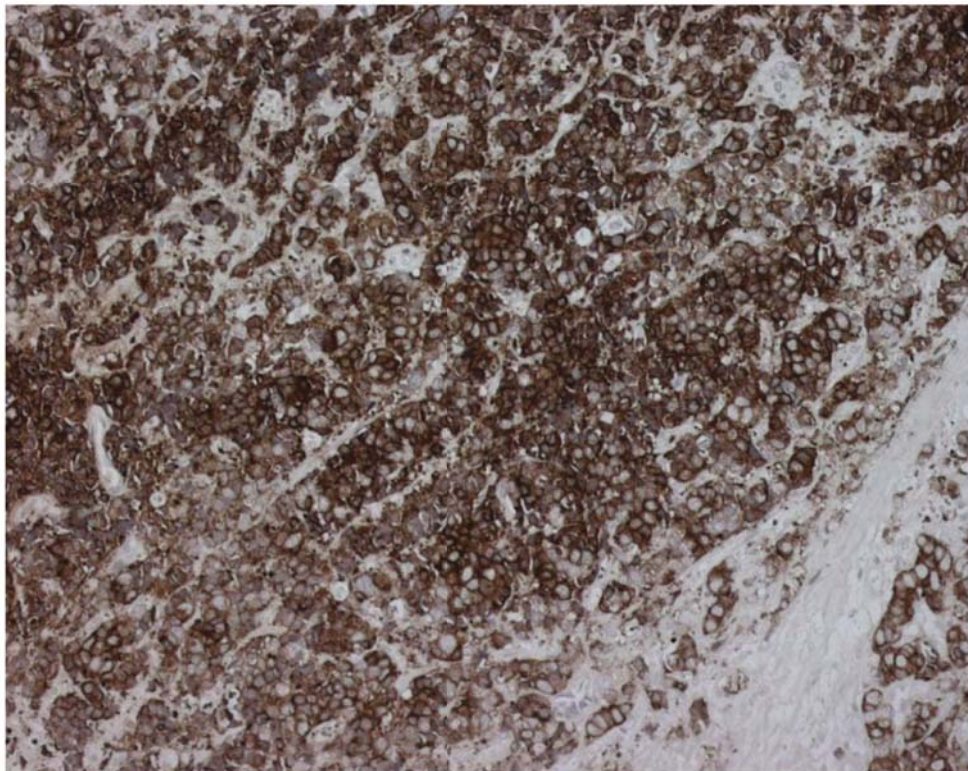


Figure 2

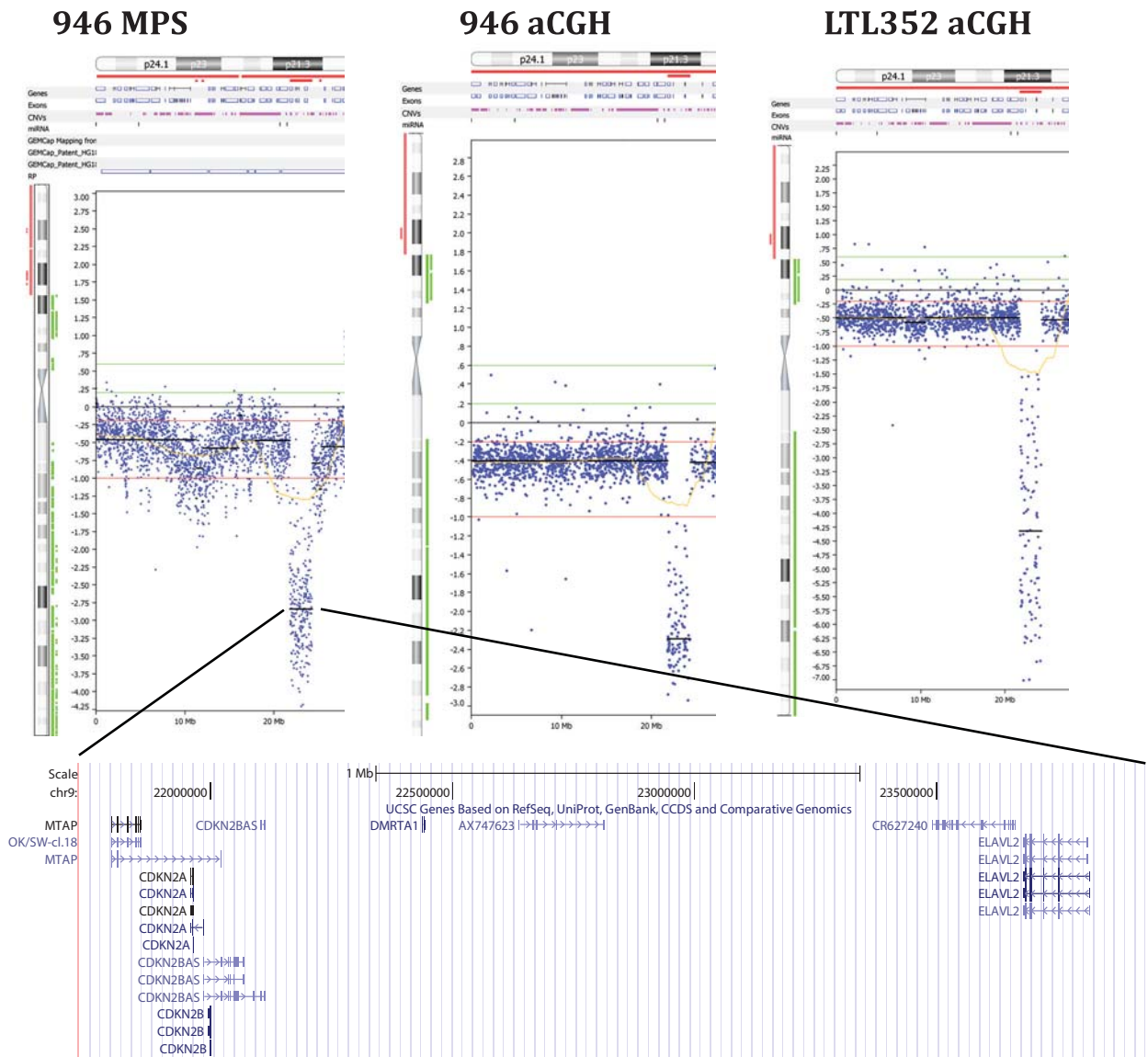
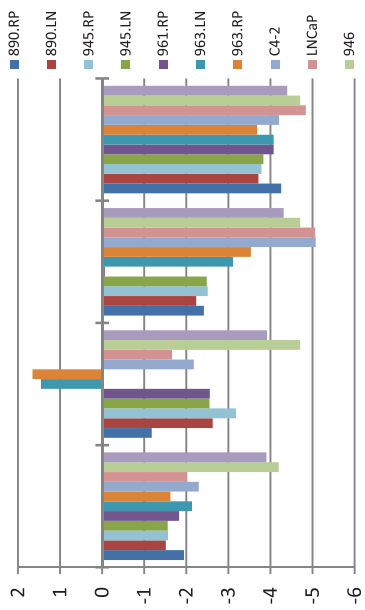
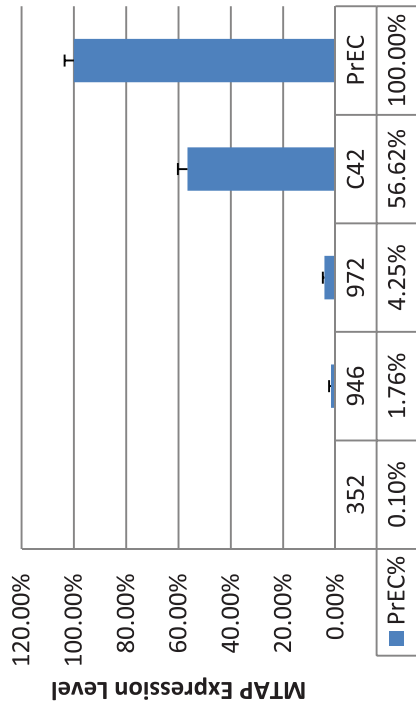


Figure 3

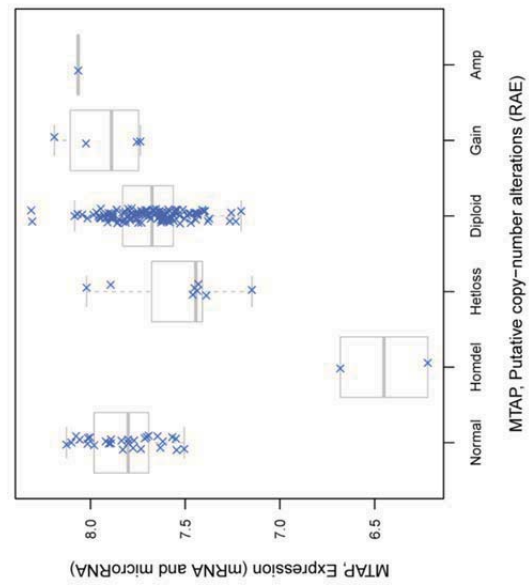
A



B



C



D

